Research Square

Preprints are preliminary reports that have not undergone peer review.
They should not be considered conclusive, used to inform clinical practice,
or referenced by the media as validated information.

Spatio-temporal temperature variability, climate regime shifts and thermal risk in Bankura and Purulia districts of West Bengal, India

Suranjana Manna
Biodiversity and Environmental Studies Research Centre, Midnapore City College (Affiliated to Vidyasagar University)
Sougata Dalal Chowdhury
Biodiversity and Environmental Studies Research Centre, Midnapore City College (Affiliated to Vidyasagar University)
Anirban Baitalik
anirbanbaitalik@gmail.com

Midnapore City College

Case Report

Keywords: ARIMA forecasting, Climate risk, Diurnal temperature range, Temperature variability, West Bengal

Posted Date: July 20th, 2026

DOI: https://doi.org/10.21203/rs.3.rs-10214955/v1

License: This work is licensed under a Creative Commons Attribution 4.0 International License. Read Full License

Additional Declarations: No competing interests reported.

Abstract

Temperature variability is a key indicator of climate change and an important determinant of regional climate risk. This study investigates long-term temperature dynamics in the Bankura-Purulia region of eastern India using maximum and minimum temperature records from 1995 to 2025. Trend analysis, change-point detection, diurnal temperature range assessment, climate-risk mapping, and ARIMA-based forecasting were employed to examine historical and future thermal behaviour. The results reveal a significant warming trend across all stations, accompanied by a climatic regime shift during 2007–2008 and an acceleration of warming in the most recent decade. A declining diurnal temperature range indicates increasing nighttime warming, while seasonal analysis identifies the strongest warming during the monsoon season. Climate-risk assessment highlights the southern and south-eastern sectors as major thermal vulnerability hotspots. Future projections suggest the persistence of elevated temperature conditions in the coming decades. The findings demonstrate that the region is undergoing a substantial thermal transition with increasing climate risk and provide a scientific basis for regional adaptation and climate-resilience planning.

Highlights

1. Persistent regional warming was observed during 1995–2025.

2. Thermal variability exhibited significant changes under a warming climate.

3. A climatic regime shift occurred during the late 2000s.

4. Temperature projections indicate continued warming in the coming decade.

5. Climate-risk hotspots were identified through integrated thermal-risk assessment.

1. Introduction

Climate change has become one of the most critical environmental challenges of the contemporary world (Steffen et al., 2022; Sultana, 2022; Abbass et al., 2022; McCulloch et al., 2024). Among the various manifestations of climate change, temperature variability is widely recognized as a fundamental indicator of alterations in the Earth's climatic system (Guo et al., 2021; Forster et al., 2023; Forster et al., 2024). Temperature reflects changes in atmospheric energy balance and influences several environmental processes, including hydrological cycles, ecosystem functioning, agricultural productivity, and human health (Yuan et al., 2024; Miralles et al., 2025). Rising air temperatures have intensified thermal extremes and heat-wave events in many parts of the world (AghaKouchak et al., 2020; Di Capua & Rahmstorf, 2023). However, temperature variability is not solely governed by atmospheric processes; it is influenced by the combined effects of natural climatic fluctuations and anthropogenic modifications of the environment.

Recent assessments indicate that global warming has intensified during the last century, with India experiencing a corresponding rise in mean temperature and increasing climatic extremes (Allan et al., 2023; Krishnan et al., 2020a). The Sixth Assessment Report of the Intergovernmental Panel on Climate Change reported that the global mean surface temperature increased by approximately 1.1°C relative to the 1850–1900 baseline period (Allan et al., 2023). This warming has contributed to more frequent thermal extremes, an increase in warm nights, and heightened climate-related risks (Clarke et al., 2022; Tavares et al., 2024). The implications of these changes extend beyond the physical environment and increasingly affect food security, water availability, urban sustainability, and public health. The country's average temperature increased by approximately 0.7°C between 1901 and 2018, and future projections indicate a substantial rise in temperature during the twenty-first century (Krishnan et al., 2020b). Studies suggest that mean temperature may increase by as much as 4.4°C by the end of the century (Chakraborty et al., 2020), while maximum temperature is projected to rise within a range of 2.5°C to 4.4°C (Bal et al., 2016).

One of the major consequences of rising temperatures is the increasing likelihood of drought occurrence. Future climate projections indicate that several regions of India may experience more frequent and severe drought events after the 2030s. Areas such as the Kangsabati River Basin, the Aravalli region, and the Bundelkhand region are projected to face multiple severe-to-extreme drought episodes under future climatic conditions (Gupta et al., 2020; Mujumdar et al., 2020; Shrestha et al., 2020; Bhatla et al., 2025; Tayyaba et al., 2025). These concerns are particularly important for dryland environments, which support more than 38% of the global population and are highly sensitive to climatic fluctuations (Huang et al., 2016; Yaning et al., 2022). Rising temperatures and increasing aridity can accelerate land degradation processes, reduce ecosystem resilience, and intensify desertification risks (Huang et al., 2016; Sun et al., 2023; Jain et al., 2024; Morán-Tejeda et al., 2026). Consequently, understanding the behaviour of temperature at regional scales has become increasingly important for assessing future climate vulnerability and adaptation needs.

Beyond changes in average temperature, recent climate research has highlighted the significance of thermal variability and temperature extremes (Goswami et al., 2018; Marx et al., 2021; van der Wiel and Bintanja, 2021; Molina et al., 2025). Variations in maximum and minimum temperatures provide important insights into the changing nature of regional climates. Rising minimum temperatures are often associated with enhanced nighttime warming, which reduces nocturnal cooling and limits thermal recovery. Such conditions can increase physiological stress on human populations and ecosystems. Another important indicator is the Diurnal Temperature Range (DTR), defined as the difference between daily maximum and minimum temperatures. Changes in DTR influence atmospheric instability, cloud formation processes, and land-atmosphere energy exchanges.

Although global and national studies have generated substantial evidence regarding long-term warming trends, climate variability is inherently spatially heterogeneous. Local climatic conditions are shaped by interactions among topography, land-use characteristics, vegetation cover, atmospheric circulation, and human activities. As a result, broad-scale climate assessments often mask significant regional differences in warming patterns and thermal extremes. Regional-scale investigations are therefore essential for identifying localized warming hotspots, understanding thermal instability, and assessing climate vulnerability under changing environmental conditions. Such analyses contribute to the development of place-specific climate adaptation and risk-management strategies (Saha et al., 2022; Datta and Behera, 2022a, 2022b).

A variety of statistical and modelling approaches have been employed to investigate long-term temperature variability. Among them, non-parametric statistical techniques have gained widespread acceptance because of their robustness in analysing hydro-climatic datasets that often violate assumptions of normality. The Mann-Kendall trend test and Sen's slope estimator have been extensively applied to detect the direction and magnitude of temperature trends (Bal et al., 2016; Chakraborty & Das, 2016; Machiwal et al., 2019; Ishaku et al., 2024). While trend analysis provides valuable information regarding long-term climatic change, recent studies have increasingly focused on identifying abrupt shifts in climate regimes. Change-point detection techniques offer an effective means of detecting sudden transitions in climatic behaviour (Militino et al., 2020). Among these methods, Pettitt's non-parametric test has been widely used to identify abrupt changes in hydro-climatic time series and evaluate temporal climate transitions (Jaiswal, 2015; Kumar et al., 2023a, b).

Alongside trend detection and change-point analysis, forecasting future temperature conditions has become an important component of climate research. Time-series models enable researchers to examine temporal dependencies within climatic datasets and estimate future trajectories of climate variables. The Auto-Regressive Integrated Moving Average (ARIMA) model has emerged as one of the most widely used forecasting techniques in climatological studies because of its ability to capture both systematic temporal patterns and stochastic variations (Shumway & Stoffer, 2017; Goswami et al., 2017; Nury et al., 2017). The model has been successfully applied in temperature projection studies to estimate future warming trends and support climate adaptation planning.

Despite significant advances in temperature trend analysis, climate regime detection, and temperature forecasting, important research gaps remain. Although numerous studies have investigated temperature trends, climatic shifts, thermal anomalies, and future projections, these components are generally examined separately. Consequently, limited attention has been given to developing an integrated framework capable of simultaneously evaluating long-term warming, thermal variability, climatic regime transitions, future temperature trajectories, and climate risk. This limitation restricts a comprehensive understanding of regional thermal vulnerability under changing climatic conditions.

The present study seeks to address this gap by developing an integrated framework for analysing regional thermal dynamics and future climate vulnerability. The specific objectives of the study are: (1) to quantify long-term trends in maximum and minimum temperatures; (2) to evaluate changes in diurnal and seasonal temperature variability; (3) to identify abrupt shifts in climatic regimes; (4) to project future temperature trajectories; and (5) to develop an integrated temperature-based climate-risk assessment framework for evaluating regional thermal vulnerability.

2. Materials and methods

2.1 Study area

The study was conducted in the Bankura and Purulia districts of western West Bengal, India (Fig. 1). Purulia district extends between 22.60°N-23.50°N latitude and 85.75°E-86.65°E longitude, while Bankura district lies between 22°38'N-23°38'N latitude and 86°36'E-87°46'E longitude. Located along the transition between the Chotanagpur Plateau and the lower Gangetic Plain, the region exhibits marked physiographic and climatic heterogeneity and is recognized as one of the drought-prone areas of eastern India. The terrain is dominated by Precambrian formations, lateritic uplands, and undulating plateaus, with elevation ranging from less than 15 m in the east to more than 700 m in the west. Major rivers, including the Damodar, Dwarakeswar, Kangsabati, and Shilabati, drain the region, although seasonal water scarcity remains common because of limited soil moisture retention and variable monsoon rainfall. The climate is tropical monsoonal, characterized by hot summers, a concentrated monsoon season, and mild winters. Summer temperatures frequently exceed 40°C, while annual rainfall averages about 1400 mm in Bankura and 1321 mm in Purulia. The strong seasonality of rainfall, coupled with recurrent drought conditions, makes the region highly sensitive to climatic variability (Hazra et al., 2017; Sarkar, 2022; Singha et al., 2023).

According to the 2011 Census, the combined population of the two districts exceeds 6.5 million, with more than 87% residing in rural areas. Agriculture is the dominant livelihood activity, making local communities highly dependent on climate-sensitive natural resources (Census of India, 2011). The combination of recurrent droughts, thermal stress, environmental vulnerability, and dependence on agriculture makes Bankura and Purulia an ideal region for examining temperature variability, climatic regime shifts, and emerging climate risks.

2.2. Study design and analytical framework

This study adopted a station-based climatological assessment framework to quantify long-term temperature variability, thermal extremes, and climate risk dynamics using daily temperature observations collected from fourteen meteorological stations during 1995–2025. The analytical workflow consisted of five sequential stages: (i) data preprocessing and quality assessment, (ii) derivation of thermal indicators, (iii) seasonal and

decadal aggregation, (iv) trend and variability analysis, and (v) climate risk assessment and forecasting. A station-wise analytical framework was adopted to capture local-scale thermal heterogeneity and reveal spatial differences in warming behaviour. Daily observations were employed to maximize the detection of thermal variability, extremes, and long-term climatic trends.

2.3 Data acquisition, quality assessment, and preprocessing

Daily maximum temperature (T_{max}) and minimum temperature (T_{min}) data for the period 1995–2025 were obtained from the India Meteorological Department (IMD). The dataset was derived from the high-resolution gridded temperature product available at a spatial resolution of 0.1° × 0.1°. To capture the spatial variability of temperature across the study area, fourteen representative grid-based stations located within and surrounding Bankura and Purulia districts were selected for analysis. A total of 11,323 daily observations spanning January 1995 to December 2025 were utilized. The dataset contained no substantial missing observations and therefore required minimal preprocessing prior to analysis. The daily records were subsequently aggregated into monthly and annual time series to facilitate the assessment of long-term temperature variability, trend detection, climatic regime shifts, and future thermal projections.

To maintain equal temporal windows during decadal analysis, observations from 2025 were excluded from decade-based assessments. Three non-overlapping decades were considered: (a) 1995–2004, (b) 2005–2014, and (c) 2015–2024. Temporal variables including year, month, season, and decade were extracted from daily records to support multi-scale climate analysis.

2.4 Derivation of thermal indicators

2.4.1 Mean temperature (daily mean temperature)

Daily mean temperature was used to represent overall atmospheric thermal conditions because it integrates daytime heating and nighttime cooling into a single climatic indicator. Mean temperature is widely applied in climate variability and warming assessments because it reduces short-term fluctuations while preserving long-term climate signals (Legg, 2021; Wilks, 2011).

$$T_{mean} = \frac{T_{max} + T_{min}}{2}$$

1

where T_{mean}= Mean temperature (°C), T_{max}= Maximum temperature (°C), T_{min}= Minimum temperature (°C)

2.4.2 Diurnal Temperature Range (DTR)

DTR was selected because it measures thermal amplitude and reflects interactions among cloud cover, radiation balance, atmospheric circulation, and land-surface processes. Variations in DTR are frequently used to assess asymmetric warming and thermal stress (Easterling et al., 1997; Braganza et al., 2004).

$$DTR = T_{max} - T_{min}$$

2

where DTR = Diurnal Temperature Range (°C), T_{max}= Daily maximum temperature, T_{min}= Daily minimum temperature

2.4.3 Seasonal and decadal aggregation

Seasonal classification followed the India Meteorological Department framework to maintain consistency with regional climatological studies: (a) Winter (January-February), (b) Pre-Monsoon (March-May), (c) Monsoon (June-September), and (d) Post-Monsoon (October-December).

Decadal aggregation was performed to minimise short-term climatic fluctuations and enhance long-term signal detection. Decadal aggregation minimises interannual climatic variability and enhances identification of persistent warming signals. Long-term averaging is widely adopted to distinguish climate change signals from short-duration variability (Wilks, 2011; Legg, 2021).

$$DTM = \frac{1}{n}\sum_{i=1}^{n} T_i$$

3

where DTM = Decadal mean temperature, T_i= Temperature observation, n= Total number of observations within the decade

2.5 Trend detection and magnitude estimation

2.5.1 Mann-Kendall trend statistic

The Mann-Kendall test was selected because climatic datasets often violate assumptions of normality and may contain outliers. This non-parametric approach is robust for environmental time series and effectively detects monotonic trends without requiring normally distributed observations (Mann, 1945; Kendall, 1975; Yue & Pilon, 2004).

$$S = \sum_{i=1}^{n-1} \sum_{j=i+1}^{n} sgn(x_j - x_i)$$

4

Sign Function:

$$sgn\,(x) = \begin{cases} 1, & x > 0 \\ 0, & x = 0 \\ -1, & x < 0 \end{cases}$$

5

where S= Mann–Kendall statistic, x_i, x_j= observations at times $i$and j, n= number of observations

2.5.2 Sen's slope estimator

Sen's slope estimator was employed because it provides robust estimates of trend magnitude and is relatively insensitive to outliers and skewed distributions. It complements Mann-Kendall testing by quantifying warming intensity (Sen, 1968; Yue & Pilon, 2004). Pairwise slope:

$$Q_i = \frac{x_j - x_i}{j - i}$$

6

Overall slope:

$$Q = Median\,(Q_i)$$

7

where Q_i= Individual pairwise slope, Q= Sen's slope estimate, x_i, x_j= observations

2.6 Climate Variability Index (CVI)

The Climate Variability Index (CVI) was used to quantify the relative variability of temperature across stations and time periods. The index is based on the conventional Coefficient of Variation (CV), which standardizes the standard deviation relative to the mean temperature and enables comparison among locations characterized by different thermal regimes. Higher CV values indicate greater climatic variability and thermal instability, whereas lower values reflect more stable temperature conditions. The coefficient of variation has been widely applied in climatological studies to evaluate temporal and spatial variations in temperature and other meteorological variables (Wilks, 2011; Legg, 2021).

$$CVI\,(CV) = \frac{\sigma}{\mu} \times 100$$

8

where CVI(CV) = Climate Variability Index (Coefficient of Variation) (%), σ = Standard deviation of temperature, μ = Mean temperature

2.7 Temperature anomaly

Temperature anomalies remove baseline climatic differences and emphasise departures from long-term normal conditions. Anomaly analysis is widely used to assess abnormal warming and thermal extremes (Legg, 2021).

$$A_i = T_i - \overset{'}{T}$$

9

where A_i= Temperature anomaly, T_i= Observed temperature, $\overset{'}{T}$= Long-term average temperature

2.8 Heatwave threshold

Percentile-based thresholds were preferred because they account for local climatic conditions and spatial variability. Station-specific thresholds are more suitable than fixed temperature cutoffs for heterogeneous climatic regions (Perkins & Alexander, 2013; Legg, 2021).

Threshold equation:

$$P_{95} = Quantile(T_{max}, 0.95)$$

10

Heatwave occurrence:

$$HW = \begin{cases} 1, & T_{max} \geq P_{95} \\ 0, & T_{max} < P_{95} \end{cases}$$

11

where HW= Heatwave occurrence, P_{95}= 95th percentile threshold

2.9 Climate Risk Index (CRI)

The integrated index approach combines warming intensity, thermal variability, and extreme heat exposure into a unified framework, allowing multidimensional climate risk assessment (Dolan & Walker, 2006; Legg, 2021). Equal weighting was adopted because no prior empirical evidence justified differential weighting among the selected indicators. Standardization ensured comparable contribution of each component to the composite index.

$$CRI = Z\left(SenSlope\right) + Z\left(Heatwave\right) + Z\left(CVI\right)$$

12

where CRI = Climate Risk Index, Z= Standardized variable, SenSlope = Trend magnitude, Heatwave = Heatwave frequency, CVI = Climatic variability

2.10 Warming rate

Warming rate expressed in °C decade⁻¹ provides a standardised measure for comparing thermal changes across stations and decades (Hartmann et al., 2013).

$$WR = \beta \times 10$$

13

where WR = Warming rate (°C decade⁻¹), where β represents Sen's slope (°C year⁻¹).

2.11 ARIMA forecasting model

ARIMA models were selected because they efficiently capture temporal autocorrelation, trend persistence, and stochastic variability in climate time series, making them suitable for temperature forecasting (Box et al., 2015).

General form:

$$ARIMA(p, d, q)$$

14

Expanded form:

$$Y_t = c + \sum_{i=1}^{p} \phi_i Y_{t-i} + \sum_{j=1}^{q} \theta_j \epsilon_{t-j} + \epsilon_t$$

15

where Y_t= Temperature at time t, p= Autoregressive order, d= Differencing order, q= Moving average order, ϵ_t= Error term

3. Results

3.1 Long-term temperature trends

The analysis of temperature records from 1995 to 2025 reveals a consistent warming trend across the Bankura-Purulia region (Fig. 2; Table 1). Annual maximum temperature increased from approximately 32.0°C during the mid-1990s to more than 32.3°C in recent years, while minimum temperature rose from about 19.1°C to 20.8°C over the same period (Figs. 2a-b). The stronger increase in minimum temperature indicates enhanced nighttime warming, a characteristic feature of contemporary climate change.

The annual mean temperature exhibited a clear upward trajectory, increasing from nearly 25.0°C during the late 1990s to over 26.5°C by 2024 (Fig. 2c). The fitted regression line confirms a persistent warming tendency throughout the study period. Temporal variations in maximum, minimum, and mean temperatures further demonstrate that warming has affected all components of the regional thermal regime (Fig. 2d).

Station-wise statistics also indicate spatially coherent warming across the study area (Table 1). Mean annual temperature varied from 25.41°C at Stations 1 and 2 to 26.84°C at Station 14. Sen's slope estimates remained positive at all monitoring stations, ranging between 0.0125 and 0.0238°C year^{-1}, while Kendall's Tau values varied from 0.256 to 0.411. The strongest warming trend was recorded at Station 3 (Sen's slope = 0.0238°C year^{-1}, $\tau = 0.402$, $p = 0.0016$), whereas Stations 6, 7, 10, and 11 exhibited comparatively lower but statistically significant warming rates of 0.0125°C year^{-1} ($p = 0.0449$).

Temperature variability remained relatively low across the region (Table 1), with coefficients of variation ranging from 1.31% to 1.75%, indicating stable thermal conditions despite the progressive rise in temperature. Furthermore, all stations recorded statistically significant positive trends ($p < 0.05$), confirming that warming is a region-wide phenomenon rather than a localized climatic anomaly. Collectively, the results demonstrate that the Bankura-Purulia region has experienced sustained and statistically significant warming during the last three decades, with increasing temperatures becoming a defining feature of the regional climate system.

Table 1
Descriptive statistics and long-term trends of temperature across weather monitoring stations in the area under study (1995–2025).

Station ID	Mean Maximum Temperature (°C)	SD Max	Mean Minimum Temperature (°C)	SD Min	Mean Temperature (°C)	CV (%)	Sen's Slope (°C/year)	Kendall's Tau	p-value
1	31.35	0.51	19.47	0.38	25.41	1.75	0.0222	0.411	0.0012
2	31.35	0.51	19.47	0.38	25.41	1.75	0.0222	0.411	0.0012
3	31.53	0.48	19.76	0.47	25.65	1.66	0.0238	0.402	0.0016
4	31.74	0.44	20.29	0.41	26.01	1.49	0.018	0.346	0.0065
5	31.74	0.44	20.29	0.41	26.01	1.49	0.018	0.346	0.0065
6	32.11	0.39	21.1	0.35	26.61	1.31	0.0125	0.256	0.0449
7	32.11	0.39	21.1	0.35	26.61	1.31	0.0125	0.256	0.0449
8	31.74	0.44	20.29	0.41	26.01	1.49	0.018	0.346	0.0065
9	31.74	0.44	20.29	0.41	26.01	1.49	0.018	0.346	0.0065
10	32.11	0.39	21.1	0.35	26.61	1.31	0.0125	0.256	0.0449
11	32.11	0.39	21.1	0.35	26.61	1.31	0.0125	0.256	0.0449
12	31.96	0.42	20.67	0.47	26.31	1.59	0.0141	0.303	0.0173
13	31.96	0.42	20.67	0.47	26.31	1.59	0.0141	0.303	0.0173
14	31.49	0.4	22.18	0.37	26.84	1.36	0.0131	0.269	0.0351

Note: SD = Standard Deviation; CV = Coefficient of Variation; Sen's Slope represents the annual rate of temperature change (°C year^{-1}); Kendall's Tau indicates the strength and direction of monotonic trends; p-values < 0.05 indicate statistically significant trends at the 95% confidence level.

3.2 Climate regime shift and decadal thermal transition

The Pettitt change-point test identified a distinct shift in the annual mean temperature series during 2007–2008 (Fig. 3). The results indicate the presence of two contrasting thermal phases within the study period. The first phase (1995–2007) was characterized by relatively lower annual mean temperatures, whereas the second phase (2008–2025) exhibited consistently higher temperature values. Prior to the detected change point, annual mean temperature generally remained below 25.6°C. Following the shift, annual temperatures increased substantially, with values frequently exceeding 26.0°C. The highest annual mean temperature recorded after the transition was approximately 26.75°C in 2010, while similarly elevated temperatures were observed during the early 2020s (Fig. 3). The regime shift was also reflected in the central tendency of the temperature series. Before the change point, the median annual mean temperature remained below 26.0°C. After the shift, the median temperature increased to approximately 26.25°C, indicating a higher thermal baseline during the latter period of observation.

Decadal statistics further support the presence of a climatic transition (Table 2). Mean temperature increased across all stations between the first (1995–2004) and third (2015–2024) decades. Stations 1 and 2 recorded an increase from 25.08°C to 25.57°C, while Station 3 increased from 25.34°C to 25.89°C. Stations 6, 7, 10, and 11 showed an increase from 26.41°C to 26.75°C. Station 14 exhibited the highest decadal mean temperature, increasing from 26.67°C during 1995–2004 to 27.03°C during 2015–2024 (Table 2).

Temperature anomaly analysis revealed a corresponding temporal shift (Fig. 6a). Negative anomalies dominated the first decade across most stations. For example, Stations 1 and 2 recorded mean anomalies of − 1.07°C during 1995–2004, while Station 3 recorded − 0.81°C. During 2015–2024, anomaly values increased substantially, reaching − 0.26°C at Station 3, 0.33°C at Stations 12 and 13, 0.60°C at Stations 6, 7, 10, and 11, and 0.88°C at Station 14 (Table 2).

The decadal trend statistics indicate that several stations displayed weak cooling tendencies during the first and second decades. However, all stations exhibited positive Sen's slope values during the most recent decade (2015–2024). The highest warming rates during this period were observed at Stations 4, 5, 8, and 9 (0.0553°C $year^{-1}$), followed by Stations 12 and 13 (0.0493°C $year^{-1}$), while Stations 1 and 2 recorded warming rates of 0.0169°C $year^{-1}$ (Table 2).

Table 2
Decadal changes in temperature and DTR (1995–2024).

Station ID	Decade	Mean Temp	SD Temp	Mean DTR	Kendall's Tau	P Value	Sen's Slope	Warming Rate	Mean Anomaly
1	1995–2004	25.08	0.12	11.71	0.16	0.59	0.015273	0.09	-1.07
	2005–2014	25.37	0.39	11.91	-0.11	0.72	-0.02362	-0.18	-0.78
	2015–2024	25.57	0.47	11.78	0.11	0.72	0.016867	0.38	-0.58
2	1995–2004	25.08	0.12	11.71	0.16	0.59	0.015273	0.09	-1.07
	2005–2014	25.37	0.39	11.91	-0.11	0.72	-0.02362	-0.18	-0.78
	2015–2024	25.57	0.47	11.78	0.11	0.72	0.016867	0.38	-0.58
3	1995–2004	25.34	0.19	11.75	-0.02	1	-0.00218	-0.01	-0.81
	2005–2014	25.66	0.43	11.94	-0.07	0.86	-0.01066	-0.1	-0.49
	2015–2024	25.89	0.41	11.53	0.16	0.59	0.037969	0.34	-0.26
4	1995–2004	25.79	0.24	11.29	-0.29	0.28	-0.04157	-0.42	-0.36
	2005–2014	25.96	0.38	11.66	-0.07	0.86	-0.01625	-0.13	-0.19
	2015–2024	26.21	0.34	11.6	0.24	0.37	0.055313	0.46	0.06
5	1995–2004	25.79	0.24	11.29	-0.29	0.28	-0.04157	-0.42	-0.36
	2005–2014	25.96	0.38	11.66	-0.07	0.86	-0.01625	-0.13	-0.19
	2015–2024	26.21	0.34	11.6	0.24	0.37	0.055313	0.46	0.06
6	1995–2004	26.41	0.15	10.82	0.11	0.72	0.008266	0.01	0.26
	2005–2014	26.63	0.36	11.19	-0.16	0.59	-0.0176	-0.19	0.48
	2015–2024	26.75	0.3	10.87	0.11	0.72	0.020109	0.14	0.6
7	1995–2004	26.41	0.15	10.82	0.11	0.72	0.008266	0.01	0.26
	2005–2014	26.63	0.36	11.19	-0.16	0.59	-0.0176	-0.19	0.48
	2015–2024	26.75	0.3	10.87	0.11	0.72	0.020109	0.14	0.6
8	1995–2004	25.79	0.24	11.29	-0.29	0.28	-0.04157	-0.42	-0.36
	2005–2014	25.96	0.38	11.66	-0.07	0.86	-0.01625	-0.13	-0.19
	2015–2024	26.21	0.34	11.6	0.24	0.37	0.055313	0.46	0.06
9	1995–2004	25.79	0.24	11.29	-0.29	0.28	-0.04157	-0.42	-0.36

Note: SD = Standard Deviation; DTR = Diurnal Temperature Range; Sen's Slope indicates the rate of temperature change; positive anomaly values represent warmer-than-average conditions.

Station ID	Decade	Mean Temp	SD Temp	Mean DTR	Kendall's Tau	P Value	Sen's Slope	Warming Rate	Mean Anomaly
	2005–2014	25.96	0.38	11.66	-0.07	0.86	-0.01625	-0.13	-0.19
	2015–2024	26.21	0.34	11.6	0.24	0.37	0.055313	0.46	0.06
10	1995–2004	26.41	0.15	10.82	0.11	0.72	0.008266	0.01	0.26
	2005–2014	26.63	0.36	11.19	-0.16	0.59	-0.0176	-0.19	0.48
	2015–2024	26.75	0.3	10.87	0.11	0.72	0.020109	0.14	0.6
11	1995–2004	26.41	0.15	10.82	0.11	0.72	0.008266	0.01	0.26
	2005–2014	26.63	0.36	11.19	-0.16	0.59	-0.0176	-0.19	0.48
	2015–2024	26.75	0.3	10.87	0.11	0.72	0.020109	0.14	0.6
12	1995–2004	26.11	0.2	11.29	-0.33	0.21	-0.03556	-0.3	-0.04
	2005–2014	26.31	0.35	11.61	-0.11	0.72	-0.021	-0.16	0.16
	2015–2024	26.48	0.31	11.18	0.2	0.47	0.049304	0.37	0.33
13	1995–2004	26.11	0.2	11.29	-0.33	0.21	-0.03556	-0.3	-0.04
	2005–2014	26.31	0.35	11.61	-0.11	0.72	-0.021	-0.16	0.16
	2015–2024	26.48	0.31	11.18	0.2	0.47	0.049304	0.37	0.33
14	1995–2004	26.67	0.15	9.17	-0.02	1	-9.10E-05	-0.06	0.52
	2005–2014	26.87	0.34	9.53	-0.16	0.59	-0.02238	-0.2	0.72
	2015–2024	27.03	0.29	9.21	0.07	0.86	0.02325	0.2	0.88

Note: SD = Standard Deviation; DTR = Diurnal Temperature Range; Sen's Slope indicates the rate of temperature change; positive anomaly values represent warmer-than-average conditions.

3.3 Decadal spatial evolution of warming patterns

Decadal analysis further demonstrated DTR compression during the recent period. At Station 3, DTR declined from 11.94°C during 2005–2014 to 11.53°C during 2015–2024, while Stations 12 and 13 decreased from 11.61°C to 11.18°C. Station 14 recorded the lowest DTR, declining from 9.53°C to 9.21°C over the same period (Fig. 4; Table 2). The reduction in DTR coincided with higher minimum temperatures across several stations. Station 14 recorded the highest mean minimum temperature (22.18°C) and the lowest mean DTR (9.27°C), whereas Stations 1 and 2 exhibited lower minimum temperatures (19.47°C) and higher DTR values (11.80°C) (Table 1). The results indicate a gradual narrowing of day–night temperature differences across the Bankura-Purulia region during the study period.

3.4 Diurnal temperature range dynamics

The analysis revealed a general decline in Diurnal Temperature Range (DTR) across the study area during 1995–2025 (Table 3). Mean DTR varied from 9.27°C at Station 14 to 11.80°C at Stations 1 and 2. Most stations exhibited negative Mann-Kendall Tau values, indicating a reduction in the difference between daytime and nighttime temperatures. Statistically significant declining trends were observed at Stations 3, 12, 13, and 14 ($p < 0.05$). The strongest decrease was recorded at Stations 12 and 13 ($\tau = -0.0495$, Sen's Slope = – 0.0000743), followed by Station 14 ($\tau = -0.0222$, Sen's Slope = – 0.0000313). In contrast, Stations 1 and 2 showed negligible positive trends ($\tau = 0.0012$).

Table 3
Spatial variability and trend characteristics of Diurnal Temperature Range (DTR) across the study region (1995–2025).

Station ID	Mean DTR	SD DTR	DTR Tau	P Value	Sen's Slope
1	11.804440	3.756888	0.001166	0.852371	0.000002
2	11.804440	3.756888	0.001166	0.852371	0.000002
3	11.742730	3.839232	-0.014070	0.024742	-0.000024
4	11.483400	3.408661	-0.002830	0.651078	-0.000004
5	11.483400	3.408661	-0.002830	0.651078	-0.000004
6	10.940270	3.378240	-0.012200	0.051540	-0.000019
7	10.940270	3.378240	-0.012200	0.051540	-0.000019
8	11.483400	3.408661	-0.002830	0.651078	-0.000004
9	11.483400	3.408661	-0.002830	0.651078	-0.000004
10	10.940270	3.378240	-0.012200	0.051540	-0.000019
11	10.940270	3.378240	-0.012200	0.051540	-0.000019
12	11.299100	3.212423	-0.049500	0.000000	-0.000074
13	11.299100	3.212423	-0.049500	0.000000	-0.000074
14	9.268553	2.942653	-0.022170	0.000405	-0.000031

Note: DTR denotes Diurnal Temperature Range. Tau and Sen's Slope were derived from the Mann–Kendall and Sen's slope trend analyses, respectively. Negative values indicate DTR contraction, while positive values indicate DTR expansion. Trends are considered statistically significant at $p < 0.05$.

3.5 Seasonal thermal behaviour and heatwave characteristics

Seasonal analysis revealed substantial differences in warming patterns across the four climatic seasons (Fig. 5). The detailed seasonal statistics are provided in Table S1. The strongest warming trend was observed during the monsoon season, where all stations recorded statistically significant positive trends ($p < 0.01$). Sen's slope values ranged from 0.030°C year^{-1} to 0.037°C year^{-1}, indicating a cumulative temperature increase of approximately 0.90°C-1.11°C between 1995 and 2024.

Spatially, winter mean temperature varied from 18.93°C in the northern part of the study area to about 21.0°C in the south (Fig. 5a). The pre-monsoon season recorded the highest seasonal temperatures, with warmer conditions concentrated in the southern and central sectors of the study area (Fig. 5b), whereas during the monsoon season the warmer zone shifted towards the south-eastern region (Fig. 5c). During the post-monsoon season, mean temperature ranged from 21.90°C to 24.15°C (Fig. 5d).

Heatwave occurrence was strongly concentrated during the pre-monsoon season, reflecting the intense thermal stress that characterizes the study area is presented in Table S1. Seasonal heatwave frequency ranged from 420 to 457 days across the monitoring stations during the study period, with the highest occurrences recorded at Stations 6, 7, 10, and 11 (457 days), followed by Station 3 (445 days) and Stations 4, 5, 8, and 9 (442 days). In contrast, heatwave events were absent during the winter and post-monsoon seasons. Monsoon-season heatwave occurrences were considerably lower, varying between 91 and 128 days. The concentration of more than 75% of total heatwave events during the pre-monsoon period indicates that extreme thermal conditions are becoming increasingly persistent before the onset of the southwest monsoon, thereby enhancing regional heat stress and climatic vulnerability.

3.6 Climate risk and thermal vulnerability

The Climate Risk Index (CRI) revealed substantial spatial variation in thermal vulnerability across the study area (Fig. 6d). The station-wise values of the integrated Climate Risk Index (CRI) are summarized in Table S2. CRI values ranged from 0.30 to 0.67, indicating the presence of both relatively low-risk and high-risk zones. The lowest CRI values (< 0.35) were concentrated in the north-western sector, whereas the highest values (> 0.60) occurred in the southern and south-eastern parts of the region.

The spatial distribution of thermal risk closely corresponded with the observed temperature anomaly patterns (Fig. 6a-b). Negative temperature anomalies dominated the earlier part of the study period, while positive anomalies became increasingly prominent after 2008 and intensified during the most recent decade. The highest anomaly values were recorded in stations located within the high-risk zone, particularly during the 2015–2024 period (Table 2).

The hotspot analysis identified several localized clusters of elevated climate risk in the southern and south-eastern sectors of the study area (Fig. 6d). These hotspot zones corresponded with higher mean annual temperatures (26.48–27.03°C), lower DTR values (9.27–11.18°C), and positive

temperature anomalies ranging from 0.33°C to 0.88°C. In contrast, stations situated within the lower-risk north-western zone exhibited comparatively lower mean temperatures (25.08–25.57°C) and predominantly negative anomaly values during the earlier decades.

The Climate Variability Index (CVI) further indicated marked interannual fluctuations in climatic conditions across the study area (Fig. 6c). Despite year-to-year variability, the overall thermal regime showed a persistent warming tendency, reflected in the progressive increase in temperature anomalies and the spatial expansion of high-risk zones. The results collectively indicate a concentration of thermal vulnerability in the southern and south-eastern parts of the Bankura-Purulia region, where elevated temperatures, positive anomalies, and higher CRI values coincide (Fig. 6d). Detailed station-level climate risk statistics are presented in Table S2.

3.7 Future thermal trajectories

The ARIMA(0,1,0) model demonstrated satisfactory forecasting performance (AIC = 27.30, RMSE = 0.363°C, MAE = 0.298°C, MAPE = 1.141%), and residual diagnostics confirmed the absence of significant autocorrelation (Ljung-Box p = 0.656), indicating that the model adequately captured the temporal structure of the annual temperature series (Fig. 7a). The complete ARIMA forecast values and their corresponding 95% prediction intervals for all weather monitoring stations are presented in Table S3. The residuals remained approximately centred around zero and exhibited a near-normal distribution, supporting the reliability of the forecasting framework.

Forecast results suggest that the warming conditions identified during the historical period are likely to persist throughout 2026–2035 (Fig. 7b). Station-wise projected temperatures for 2026–2035 are provided in Table S3. Projected mean temperatures range from 25.85°C at Stations 1 and 2 to 26.84°C at Station 14, while several stations are expected to maintain temperatures above 26.50°C during the forecast horizon. The 95% prediction intervals widen gradually with increasing lead time, reflecting greater uncertainty in long-term projections. For example, the forecast range at Station 1 expands from 25.03–26.67°C in 2026 to 23.26–28.45°C by 2035. Despite this uncertainty, projected temperatures remain consistently above the cooler conditions observed during the late 1990s and broadly correspond to the warmer climatic regime established after the 2007–2008 shift. The results indicate the continued persistence of elevated thermal conditions across the Bankur-Purulia region over the coming decade.

4. Discussion

The findings reveal that the Bankura-Purulia region has experienced a persistent warming trend during 1995–2025, indicating a substantial modification of the regional thermal regime. The positive temperature trends recorded across all stations suggest that warming is spatially pervasive rather than localized. Similar warming patterns have been documented across India, where increases in annual mean, maximum, and minimum temperatures have been attributed to the combined influence of greenhouse-gas forcing, land-use transformation, and changing land-atmosphere interactions (Ray et al., 2019; Sanjay et al., 2020). Recent assessments further indicate that semi-arid and plateau regions are particularly sensitive to rising temperatures because of their limited moisture availability and high evaporative demand (Krishnan et al., 2020b). The warming observed in Bankura and Purulia therefore reflects both broader climatic changes occurring across India and the inherent environmental sensitivity of the western plateau fringe of West Bengal.

A notable outcome of the study is the identification of a significant climatic regime shift around 2007–2008. The abrupt transition from a relatively cooler phase to a persistently warmer thermal regime indicates that climate change in the region has not evolved solely through gradual warming but also through structural reorganization of the climatic system. Similar regime shifts have been reported across India, particularly during the late twentieth century, where abrupt changes in temperature-related indices were associated with large-scale atmospheric and climatic adjustments (Soorya Gayathri et al., 2023; Sankaran et al., 2024). Recent evidence also suggests that climatic non-stationarity and regime transitions have become increasingly prominent across India under ongoing global warming (Aruna et al., 2026). The persistence of elevated temperatures after the detected change point indicates that the regional climate has entered a new thermal state characterized by higher baseline temperatures and greater climatic stress.

The decline in diurnal temperature range (DTR) observed across most stations provides further evidence of changing thermal characteristics. Negative DTR trends indicate that minimum temperatures are increasing more rapidly than maximum temperatures, resulting in enhanced nighttime warming. Similar asymmetric warming has been reported across India, where reductions in DTR have been linked to increased atmospheric moisture, cloud cover, urbanization, and enhanced long-wave radiation trapping (Oza & Kishtawal, 2015; Mall et al., 2021). Studies from the Sutlej Basin and other regions of India have likewise shown that rising minimum temperatures constitute a major component of contemporary climate change (Singh et al., 2015; Sonali & Kumar, 2016). In drought-prone environments such as Bankura and Purulia, declining DTR may intensify thermal stress by limiting nocturnal cooling and increasing cumulative heat exposure.

Seasonal analysis demonstrated that monsoon temperatures exhibited the strongest warming signal. This finding is particularly important because the southwest monsoon traditionally moderates thermal conditions across eastern India. Similar monsoon-season warming has been reported at national and regional scales, where rising temperatures during the monsoon have been associated with increasing atmospheric instability and changing moisture-energy dynamics (Ray et al., 2019; Das & Goswami, 2023). The simultaneous occurrence of significant monsoon warming and frequent pre-monsoon heatwave conditions suggests an expansion of thermal stress across a larger portion of the annual climatic cycle. Such

changes may increase evapotranspiration losses, alter soil-moisture dynamics, and reduce agricultural resilience in a region already characterized by recurrent drought and water scarcity (Hazra et al., 2017; Ghosh, 2019).

The spatial pattern of climate risk highlights considerable heterogeneity in thermal vulnerability. Higher Climate Risk Index values were concentrated in the southern and south-eastern sectors of the study area, where elevated temperatures, stronger anomalies, and lower DTR values occurred simultaneously. This pattern supports the argument that climate vulnerability emerges from the interaction between warming intensity, thermal variability, and environmental sensitivity rather than from temperature increase alone. Previous investigations in Bankura and Purulia have similarly identified drought-prone sectors characterized by greater climatic stress, agricultural vulnerability, and water-resource constraints (Senapati et al., 2021; Goswami et al., 2023). The coincidence of warming hotspots and drought-sensitive landscapes suggests that future climate impacts may be disproportionately concentrated within these sectors.

The projected continuation of warming derived from ARIMA modelling indicates that current thermal trends are likely to persist in the coming decades. Although the projected increase appears moderate, climate literature consistently demonstrates that even small increases in mean temperature substantially increase the probability, duration, and intensity of extreme heat events (Maurya et al., 2024; Prajapat et al., 2025). Future warming may therefore intensify drought occurrence, increase atmospheric water demand, and amplify heat-related risks for agriculture, ecosystems, and rural livelihoods. This concern is particularly relevant for Bankura and Purulia, where recurrent drought, rainfall variability, and dependence on climate-sensitive agriculture already constrain adaptive capacity (Das & Tahir, 2026; Hazra et al., 2017).

Climate change in the western plateau fringe of West Bengal is manifested through interconnected processes of sustained warming, climatic regime shifts, declining diurnal temperature range, intensified seasonal warming, and spatially differentiated climate risk. These findings support emerging evidence that regional climate systems are increasingly characterized by non-linear thermal transformations rather than simple temperature increases alone. The convergence of these processes suggests that Bankura and Purulia are entering a period of heightened climatic vulnerability, emphasizing the need for region-specific adaptation strategies, climate-resilient water management, and long-term monitoring of thermal extremes to strengthen resilience under future climate change.

5. Conclusions

The present study demonstrates that the Bankura-Purulia region has experienced a substantial transformation in its thermal regime over recent decades, characterized by persistent warming, shifts in temperature behaviour, changes in diurnal thermal patterns, and increasing climatic variability. The emergence of a warmer climatic phase, accompanied by seasonal disparities in warming intensity and spatial differences in vulnerability, highlights the growing influence of climate change on this drought-prone transitional landscape. The identification of thermal hotspots and the persistence of elevated future temperature conditions indicate that climatic risks are becoming increasingly concentrated across specific parts of the region. The study provides a comprehensive understanding of regional climate dynamics and establishes a scientific basis for strengthening climate resilience, environmental planning, and long-term adaptation strategies in the western plateau fringe of West Bengal.

Limitations of the study

This study focuses primarily on temperature-based indicators and therefore does not capture the influence of other climatic variables that may affect regional climate risk. The analysis is based on gridded temperature data, which may overlook localized thermal variations. In addition, the climate-risk assessment emphasizes thermal conditions and does not explicitly incorporate socioeconomic dimensions of vulnerability. Future studies integrating higher-resolution climatic and socio-environmental datasets could provide a more comprehensive understanding of regional climate change impacts.

Declarations

Supplementary file

https://docs.google.com/document/d/1QcgMw0OmNx_UsI604SqUuHgSWZ-1dC1-/edit?usp=sharing&ouid=110329660980723061857&rtpof=true&sd=true

CRediT authorship contribution statement

SM: Conceptualization, methodology, data mining, analysis, visualization, and manuscript drafting. **SDC**: Formal analysis and review. **AB**: Supervision and manuscript review.

Declaration of competing interest

The authors declare that there are no financial or personal conflicts of interest that could have influenced the research findings or interpretations presented in this study.

Ethical approval and consent to participate

Not applicable.

Consent for publication

All authors have read and approved the final version of the manuscript and consent to its publication.

Funding

The authors did not receive any financial support for this work.

Author Contribution

SM: Conceptualization, methodology, data mining, analysis, visualization, and manuscript drafting. SDC: Formal analysis and review. AB: Supervision and manuscript review.

Acknowledgement

The authors sincerely acknowledge the Research Centre of Biodiversity and Environmental Studies at Midnapore City College (affiliated to Vidyasagar University), for academic support and research facilities. The authors also extend their gratitude to the pioneering scholars whose contributions laid the groundwork for this study.

Data availability

All data and materials used or analyzed in this study can be obtained from the corresponding author upon reasonable request.

References

1. Abbass K, Qasim MZ, Song H, Murshed M, Mahmood H, Younis I (2022) A review of the global climate change impacts, adaptation, and sustainable mitigation measures. Environ Sci Pollut Res 29(28):42539–42559
2. AghaKouchak A, Chiang F, Huning LS, Love CA, Mallakpour I, Mazdiyasni O, Sadegh M (2020) Climate extremes and compound hazards in a warming world. Annu Rev Earth Planet Sci 48(1):519–548
3. Allan RP, Arias PA, Berger S, Canadell JG, Cassou C, Chen D, Zickfeld K (2023) Intergovernmental panel on climate change (IPCC). Summary for policymakers. In Climate change 2021: The physical science basis. Contribution of working group I to the sixth assessment report of the intergovernmental panel on climate change (pp. 3–32). Cambridge University Press
4. Aruna M, Bharghavi K, Reddy TL, Reddy KK (2026) Evolving thermodynamic convective environments over India: spatio-temporal variability, trends, and regime shifts. Evol Earth, 100132
5. Bal PK, Ramachandran A, Palanivelu K, Thirumurugan P, Geetha R, Bhaskaran B (2016) Climate change projections over India by a downscaling approach using PRECIS. Asia-Pac J Atmos Sci 52:353–369
6. Bhatla R, Verma A, Vishwakarma A, Mall RK (2025) India's Drought Challenge: Insights From CMIP6 Models on Historical and Future Climate Scenarios. Int J Climatol, 45(13), e70075
7. Box GE, Jenkins GM, Reinsel GC, Ljung GM (2015) Time series analysis: forecasting and control. Wiley
8. Braganza K, Karoly DJ, Arblaster JM (2004) Diurnal temperature range as an index of global climate change during the twentieth century. Geophys Res Lett, 31(13)
9. Census of India, Population census (2011) The Registrar General & Census Commissioner, Ministry of Home Affairs, Government of India, New Delhi, India
10. Chakraborty PK, Das L (2016) Rainfall trend analysis and its future projection over Gangetic West Bengal (GWB) region of India during post-monsoon and winter season. J Appl Nat Sci 8(3):1152–1156
11. Chakraborty S, Kulkarni A, Mujumdar M, Gnanaseelan C, Sanjay J, Krishnan R (2020) Assessment of Climate Change over the Indian Region. Springer Nature
12. Clarke B, Otto F, Stuart-Smith R, Harrington L (2022) Extreme weather impacts of climate change: an attribution perspective. Environ Research: Clim 1(1):012001
13. Das S, Goswami K (2023) Unraveling the dynamics of climate: empirical evidence from the Indian state of West Bengal. J Water Clim Change 14(11):4068–4083
14. Das S, Tahir M (2026) Analysing trends of climatic variables in Purulia district, India using non-parametric methods. Discover Geoscience 4(1):84

15. Datta P, Behera B (2022) Assessment of adaptive capacity and adaptation to climate change in the farming households of Eastern Himalayan foothills of West Bengal, India. Environ Challenges 7:100462
16. Datta P, Behera B (2022) Climate change and Indian agriculture: A systematic review of farmers' perception, adaptation, and transformation. Environ Challenges 8:100543
17. Di Capua G, Rahmstorf S (2023) Extreme weather in a changing climate. Environ Res Lett 18(10):102001
18. Dolan AH, Walker IJ (2006) Understanding vulnerability of coastal communities to climate change related risks. J Coastal Res, 1316–1323
19. Easterling DR, Horton B, Jones PD, Peterson TC, Karl TR, Parker DE, Folland CK (1997) Maximum and minimum temperature trends for the globe. Science 277(5324):364–367
20. Forster PM, Smith CJ, Walsh T, Lamb WF, Lamboll R, Hauser M, Zhai P (2023) Indicators of Global Climate Change 2022: annual update of large-scale indicators of the state of the climate system and human influence. Earth Syst Sci data 15(6):2295–2327
21. Forster PM, Smith C, Walsh T, Lamb WF, Lamboll R, Hall B, Zhai P (2024) Indicators of Global Climate Change 2023: annual update of key indicators of the state of the climate system and human influence. Earth Syst Sci Data 16(6):2625–2658
22. Ghosh KG (2019) Spatial and temporal appraisal of drought jeopardy over the Gangetic West Bengal, eastern India. Geoenvironmental Disasters 6(1):1–21
23. Goswami K, Hazarika J, Patowary AN (2017) Monthly temperature prediction based on arima model: A case study in dibrugarh station of assam, india. Int J Adv Res Comput Sci 8(8):292–298
24. Goswami S, Mahato S, Mahato S, Kundu A, Bairwa B, Chattoraj KK, Siddiqui AR (2023) Evaluating Agricultural Drought in the Purulia District, West Bengal (India): An Earth Observation Perspective. Agriculture and Climatic Issues in South Asia. CRC, pp 114–128
25. Goswami UP, Bhargav K, Hazra B, Goyal MK (2018) Spatiotemporal and joint probability behavior of temperature extremes over the Himalayan region under changing climate. Theoretical Appl Climatology 134(1–2):477
26. Guo F, Do V, Cooper R, Huang Y, Zhang P, Ran J, Fu Z (2021) Trends of temperature variability: Which variability and what health implications? Sci Total Environ 768:144487
27. Gupta V, Kumar Jain M, Singh VP (2020) Multivariate modeling of projected drought frequency and hazard over India. J Hydrol Eng 25(4):04020003
28. Hartmann DL, Tank AMK, Rusticucci M, Alexander LV, Brönnimann S, Charabi YAR, Zhai P (2013) Observations: atmosphere and surface. Climate Change 2013–The Physical Science Basis. Cambridge University Press, pp 159–254
29. Hazra S, Roy S, Mitra S (2017) Enhancing adaptive capacity and increasing resilience of small and marginal farmers of Purulia and Bankura districts, West Bengal to climate change. DRCSC report, 1114
30. Huang J, Yu H, Guan X, Wang G, Guo R (2016) Accelerated dryland expansion under climate change. Nat Clim change 6(2):166–171
31. Ishaku D, Umaru ET, Adebayo AA, Löwner R, Okhimamhe AA (2024) Analysis of the observed trends in rainfall and temperature patterns in North-Eastern Nigeria. Climate 12(12):219
32. Jain S, Srivastava A, Khadke L, Chatterjee U, Elbeltagi A (2024) Global-scale water security and desertification management amidst climate change. Environ Sci Pollut Res 31(49):58720–58744
33. Jaiswal RK, Lohani AK, Tiwari HL (2015) Statistical analysis for change detection and trend assessment in climatological parameters. Environ Processes 2(4):729–749
34. Kendall MG (1975) Rank correlation methods, 4th edn. Charles Griffin
35. Krishnan R, Gnanaseelan C, Sanjay J, Swapna P, Dhara C, Sabin TP, Niyogi D (2020a) Introduction to climate change over the Indian region. Assessment of climate change over the Indian region: A report of the Ministry of Earth Sciences (MoES), Government of India. Springer Singapore, Singapore, pp 1–20
36. Krishnan R, Sanjay J, Gnanaseelan C, Mujumdar M, Kulkarni A, Chakraborty S (2020b) Assessment of climate change over the Indian region. A Report of the Ministry of Earth Sciences (MoES). Government India, 13–17
37. Kumar A, Kumar S, Rautela KS, Kumari A, Shekhar S, Thangavel M (2023a) Exploring temperature dynamics in Madhya Pradesh: a spatial-temporal analysis. Environ Monit Assess 195(11):1313
38. Kumar S, Ahmed SA, Karkala J (2023b) Time series data and rainfall pattern subjected to climate change using non-parametric tests over a vulnerable region of Karnataka, India. J Water Clim Change 14(5):1532–1550
39. Legg S (2021) IPCC, 2021: Climate change 2021-the physical science basis. Interaction 49(4):44–45
40. Machiwal D, Gupta A, Jha MK, Kamble T (2019) Analysis of trend in temperature and rainfall time series of an Indian arid region: comparative evaluation of salient techniques. Theoret Appl Climatol 136(1):301–320
41. Mall RK, Chaturvedi M, Singh N, Bhatla R, Singh RS, Gupta A, Niyogi D (2021) Evidence of asymmetric change in diurnal temperature range in recent decades over different agro-climatic zones of India. Int J Climatol 41(4):2597–2610
42. Mann HB (1945) Nonparametric tests against trend. Econometrica 13(3):245–259
43. Marx W, Haunschild R, Bornmann L (2021) Heat waves: a hot topic in climate change research. Theoret Appl Climatol 146(1):781–800

44. Maurya HK, Joshi N, Suryavanshi S (2024) Change in high-temperature intensity-duration-frequency under different warming scenarios over India. Atmos Res 309:107567
45. McCulloch MT, Winter A, Sherman CE, Trotter JA (2024) 300 years of sclerosponge thermometry shows global warming has exceeded 1.5 C. Nat Clim Change 14(2):171–177
46. Militino AF, Moradi M, Ugarte MD (2020) On the performances of trend and change-point detection methods for remote sensing data. Remote Sens 12(6):1008
47. Miralles DG, Vilà-Guerau de Arellano J, McVicar TR, Mahecha MD (2025) Vegetation–climate feedbacks across scales. Ann N Y Acad Sci 1544(1):27–41
48. Molina MO, Soares PMM, Lima MM, Gaspar TH, Lima DCA, Ramos AM, Trigo RM (2025) Updated insights on climate change-driven temperature variability across historical and future periods. Clim Change 178(5):97
49. Morán-Tejeda E, Pricope N, Spinoni J, Toreti A, Ocampo-Melgar A, Vicente-Serrano SM (2026) Aridification impacts and adaptation strategies in the world's drylands: a review. Environ Reviews 34:1–23
50. Mujumdar M, Bhaskar P, Ramarao MVS, Uppara U, Goswami M, Borgaonkar H, Niyogi D (2020) Droughts and floods. Assessment of climate change over the Indian region: a report of the Ministry of Earth Sciences (MoES), Government of India. Springer Singapore, Singapore, pp 117–141
51. Nury AH, Hasan K, Alam MJB (2017) Comparative study of wavelet-ARIMA and wavelet-ANN models for temperature time series data in northeastern Bangladesh. J King Saud University-Science 29(1):47–61
52. Oza M, Kishtawal CM (2015) Spatio-temporal changes in temperature over India. Curr Sci, 1154–1158
53. Prajapat DK, Choudhary M, Avtar R, Singh S, Alsulamy S, Kharrazi A (2025) Transformative Spatio-Temporal Insights into Indian Summer Days for Advancing Climate Resilience and Regional Adaptation in India. Earth 6(2):39
54. Ray LK, Goel NK, Arora M (2019) Trend analysis and change point detection of temperature over parts of India: LK Ray. Theoret Appl Climatol 138(1):153–167
55. Saha S, Chakraborty D, Hazarika S, Shakuntala I, Das B, Chhabra A, Mishra VK (2022) Spatiotemporal variability of weather extremes over eastern India: evidences of ascertained long-term trend persistence and effective global climate controls. Theoret Appl Climatol 148(1):643–659
56. Sanjay J, Revadekar JV, Ramarao MVS, Borgaonkar H, Sengupta S, Kothawale DR, Ratnam JV (2020) Temperature changes in India. Assessment of climate change over the Indian region: a report of the Ministry of Earth Sciences (MoES), Government of India. Springer Singapore, Singapore, pp 21–45
57. Sankaran A, Madhusudanan SG, Ndehedehe C, Nair ANGR (2024) Spatio-temporal variability of trends in extreme climatic indices across India. KSCE J Civ Eng 28(6):2537–2551
58. Sarkar A (2022) Assessment of soil geomorphological character and its impact on land use of the hills of Purulia and Bankura districts of West Bengal, India (No. ICG2022-331). Copernicus Meetings
59. Sen PK (1968) Estimates of regression coefficient based on Kendall's tau. J Am Stat Assoc 63(324):1379–1389
60. Senapati U, Raha S, Das TK, Gayen SK (2021) A composite assessment of agricultural drought susceptibility using analytic hierarchy process: Case study of western region of West Bengal. Agriculture, food and nutrition security: A study of availability and sustainability in India. Springer International Publishing, Cham, pp 15–40
61. Shrestha A, Rahaman MM, Kalra A, Jogineedi R, Maheshwari P (2020) Climatological drought forecasting using bias corrected CMIP6 climate data: A case study for India. Forecasting 2(2):59–84
62. Shumway RH, Stoffer DS (2017) ARIMA models. Time series analysis and its applications: with R examples. Springer International Publishing, Cham, pp 75–163
63. Singh D, Glupta RD, Jain SK (2015) Statistical analysis of long term spatial and temporal trends of temperature parameters over Sutlej river basin, India. J Earth Syst Sci 124(1):17–35
64. Singha A, Pramanick N, Acharyya R (2023), April Implication of applying IPCC AR4 and AR5 framework for drought-based vulnerability and risk assessment in bankura and purulia districts, West Bengal. In IOP Conference Series: Earth and Environmental Science (Vol. 1164, No. 1, p. 012009). IOP Publishing
65. Sonali P, Nagesh Kumar D (2016) Spatio-temporal variability of temperature and potential evapotranspiration over India. J Water Clim change 7(4):810–822
66. Soorya Gayathri M, Adarsh S, Shehinamol K, Nizamudeen Z, Lal MR (2023) Evaluation of change points and persistence of extreme climatic indices across India. Nat Hazards 116(2):2747–2759
67. Steffen W, Persson Å, Deutsch L, Zalasiewicz J, Williams M, Richardson K, Svedin U (2022) The anthropocene: From global change to planetary stewardship (2011). Paul J. Crutzen and the anthropocene: A new epoch in earth's history. Springer International Publishing, Cham, pp 145–174
68. Sultana F (2022) Critical climate justice. Geographical J 188(1):118–124
69. Sun C, Feng X, Fu B, Ma S (2023) Desertification vulnerability under accelerated dryland expansion. Land Degrad Dev 34(7):1991–2004

70. Tavares C, Pereira RS, Bonnin C, Duarte D, Mills G, Morakinyo TE, Holloway P (2024) A global (South) collective burden: A systematic review of the current state of climate-related hazards in informal settlements. Int J Disaster Risk Reduct 114:104940
71. Tayyaba S, Puppala H, Arora MK (2025) Foreseeing drought-prone regions in India under climate change: a comprehensive analysis through the development of Drought Prone Index. Environ Monit Assess 197(8):866
72. van der Wiel K, Bintanja R (2021) Contribution of climatic changes in mean and variability to monthly temperature and precipitation extremes. Commun Earth Environ 2(1):1
73. Wilks DS (2011) Statistical methods in the atmospheric sciences, vol 100. Academic
74. Yaning C, Yupeng L, Zhi L, Yongchang LIU, Wenjing HUANG, Xigang LIU, Meiqing F (2022) Analysis of the impact of global climate change on dryland areas. Adv Earth Sci 37(2):111 E. N. G
75. Yuan X, Li S, Chen J, Yu H, Yang T, Wang C, Ao X (2024) Impacts of global climate change on agricultural production: a comprehensive review. Agronomy 14(7):1360
76. Yue S, Pilon P (2004) A comparison of the power of the t test, Mann-Kendall and bootstrap tests for trend detection: Detecting change in hydrological data. Hydrol Sci J 49(1):21–37

Figures

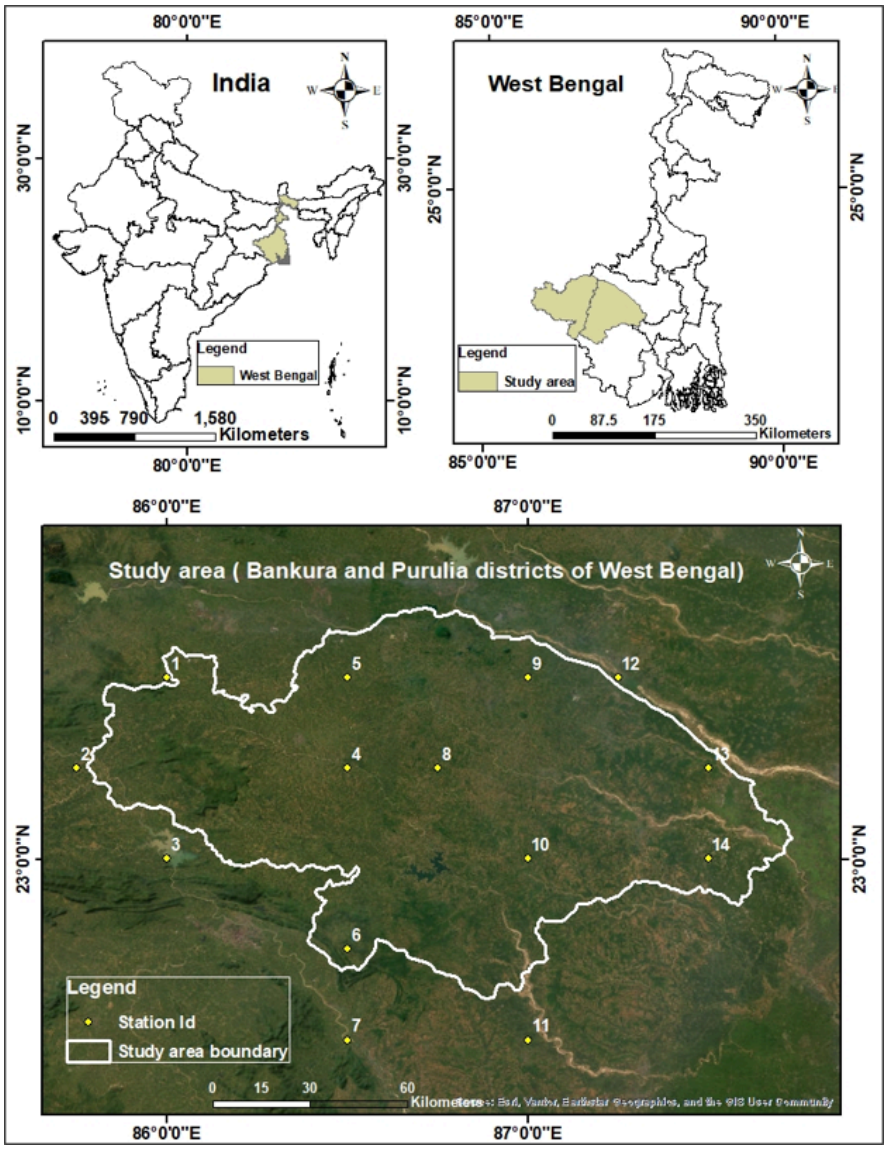


Figure 1

Study area and spatial configuration of weather monitoring stations.

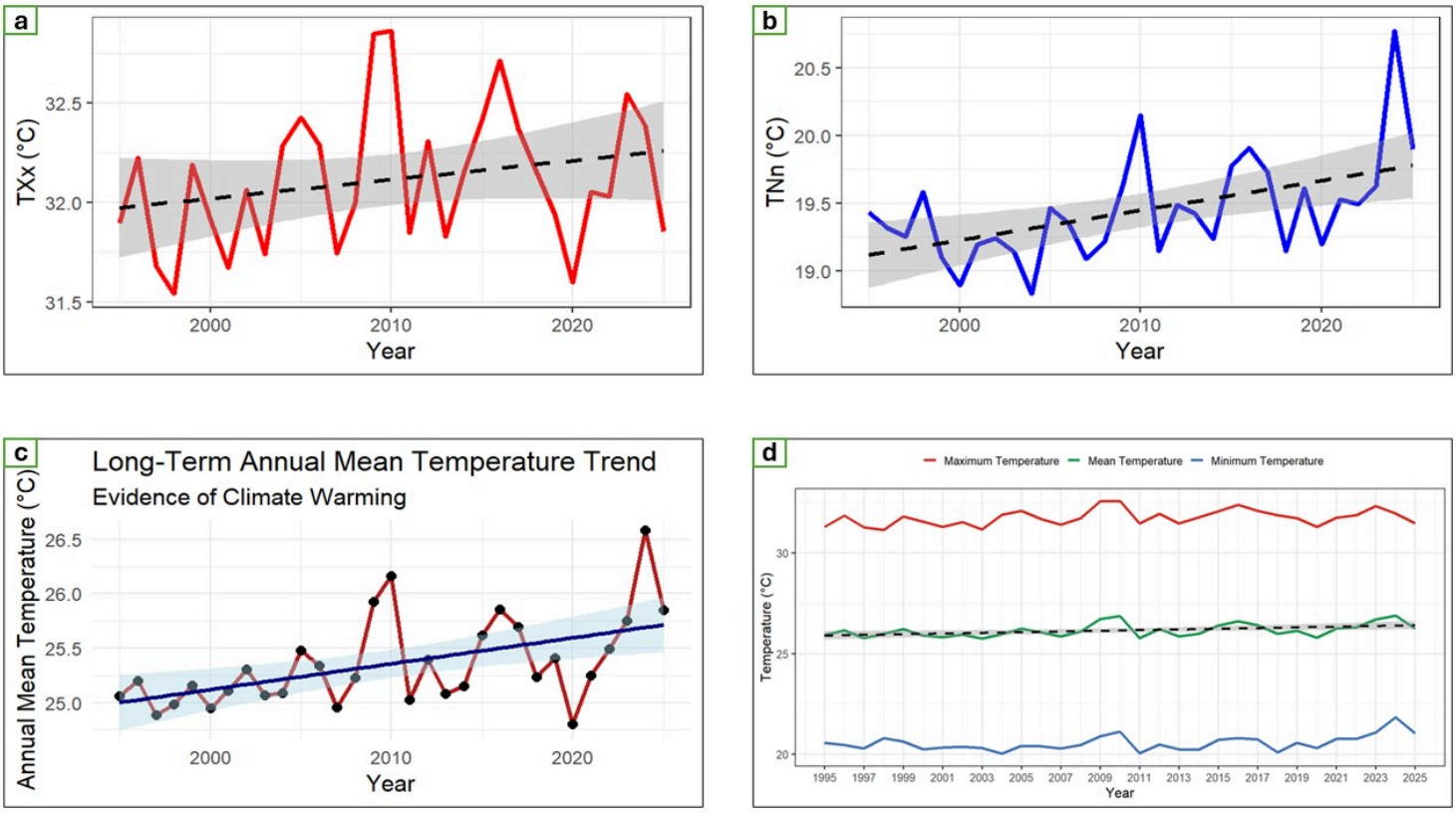


Figure 2

Long-term temperature variability and warming trends in the Bankura–Purulia region during 1995-2025. (a) Annual maximum temperature trend; (b) annual minimum temperature trend; (c) annual mean temperature trend with fitted linear regression line; and (d) temporal variation of maximum, minimum, and mean temperatures. Dashed lines indicate linear trend estimates, while shaded areas represent 95% confidence intervals around the fitted trends.

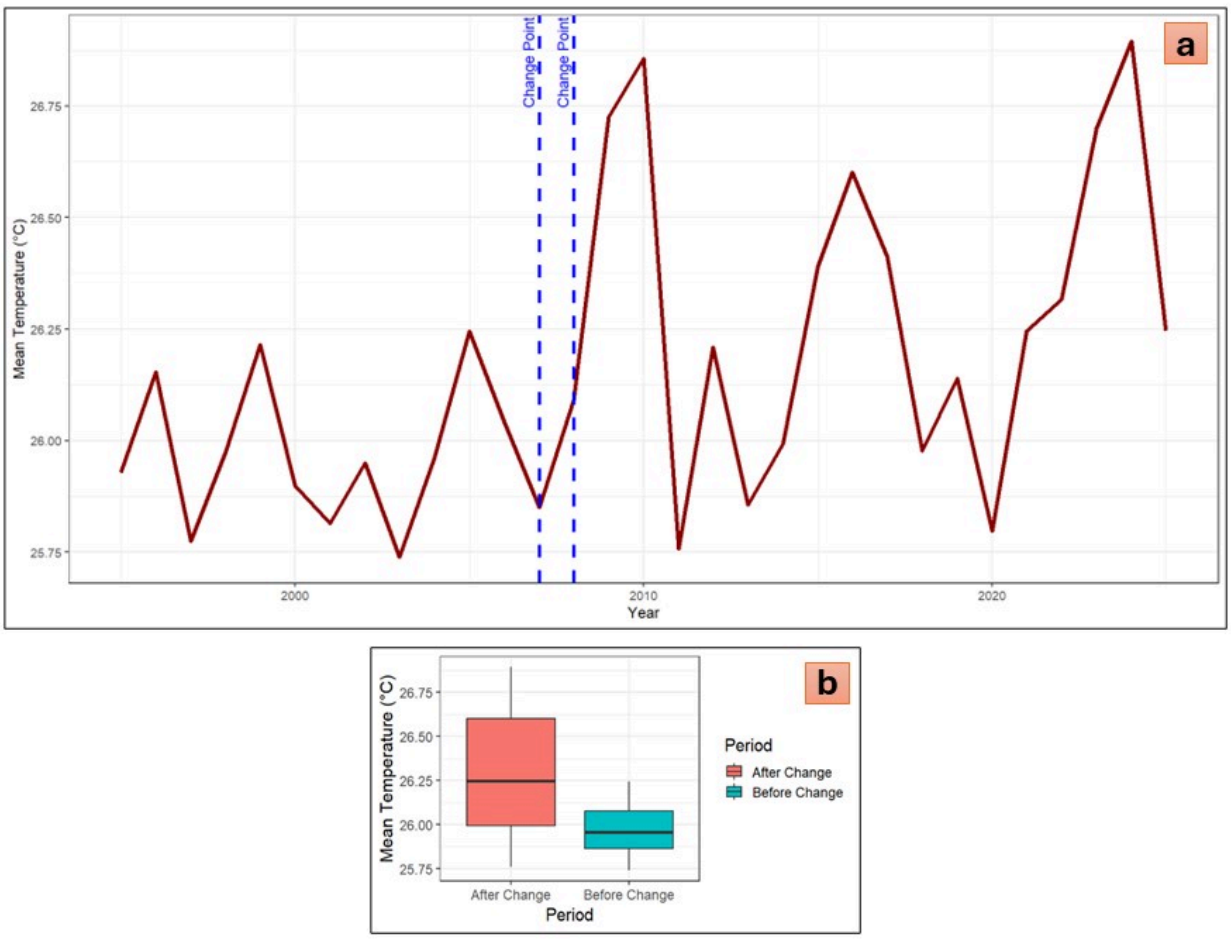


Figure 3

Change point detection and regime shift for annual mean temperature (a) Pettitt Change Point Detection (the dashed blue vertical line marking the changing climate regime). (b). Boxplot showing the distribution, median, and variability of annual mean temperatures before and after the changing point.

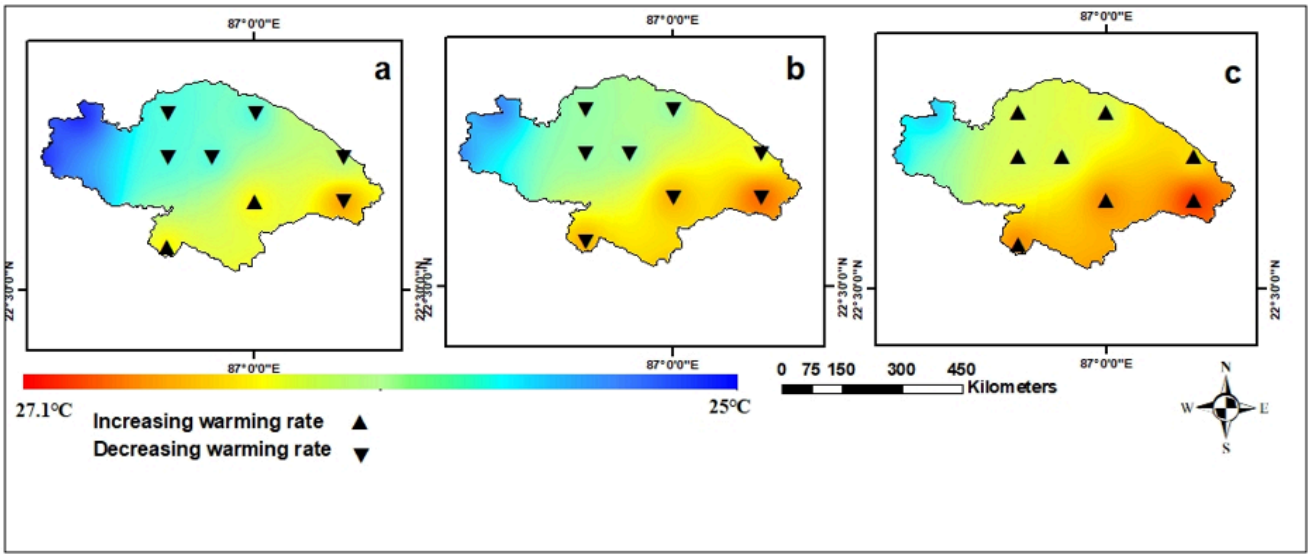


Figure 4

Spatial distribution of mean temperature and warming-rate trends during (a) 1995-2004, (b) 2005-2014, and (c) 2015-2024. Upward triangles indicate increasing warming rates, whereas downward triangles represent decreasing warming rates.

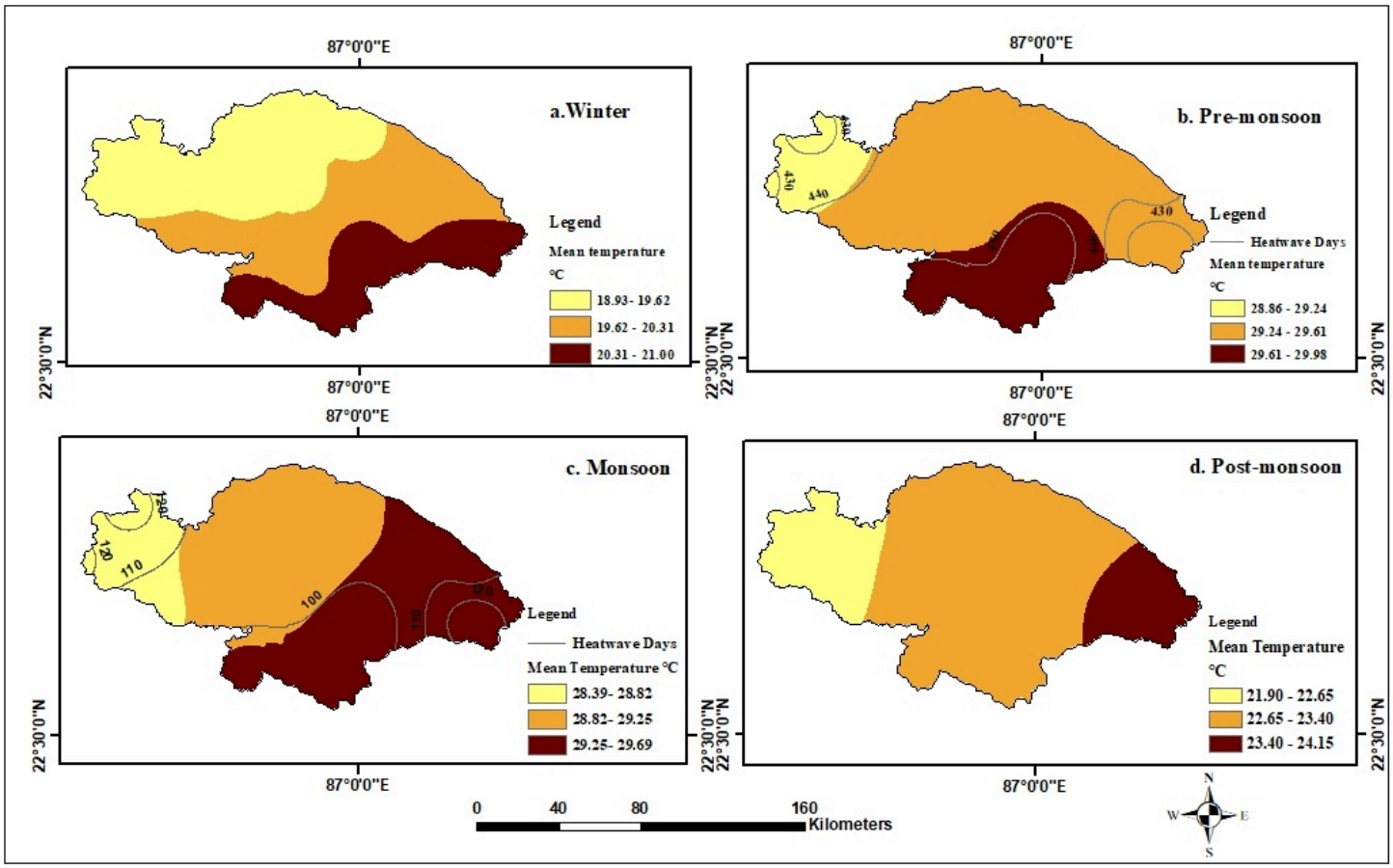


Figure 5

Spatial distribution of seasonal mean temperature and heatwave conditions across the Bankura-Purulia districts during (a) winter (January-February), (b) pre-monsoon (March-May), (c) monsoon (June-September), and (d) post-monsoon (October-December) seasons.

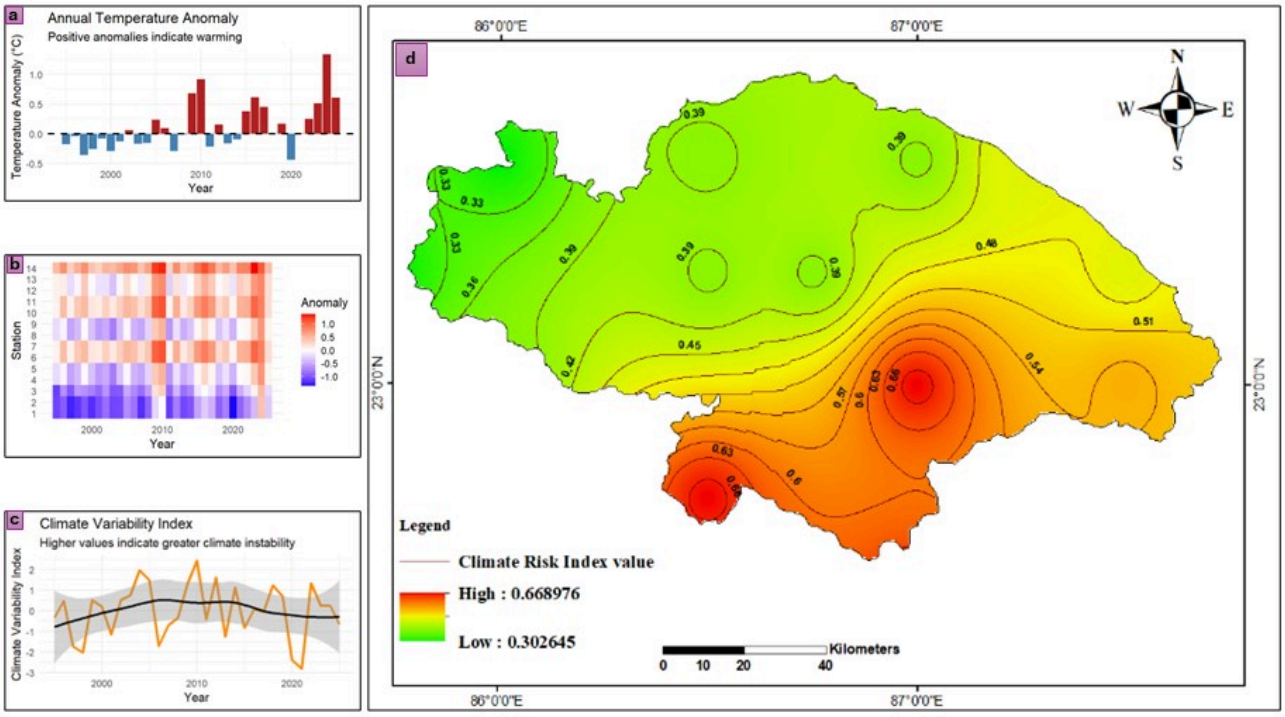


Figure 6

Integrated assessment of regional thermal dynamics showing (a) annual temperature anomalies, (b) spatio-temporal distribution of station-wise temperature anomalies, (c) temporal variation in climate variability, and (d) spatial distribution of the Climate Risk Index (CRI) across the Bankura-Purulia region.

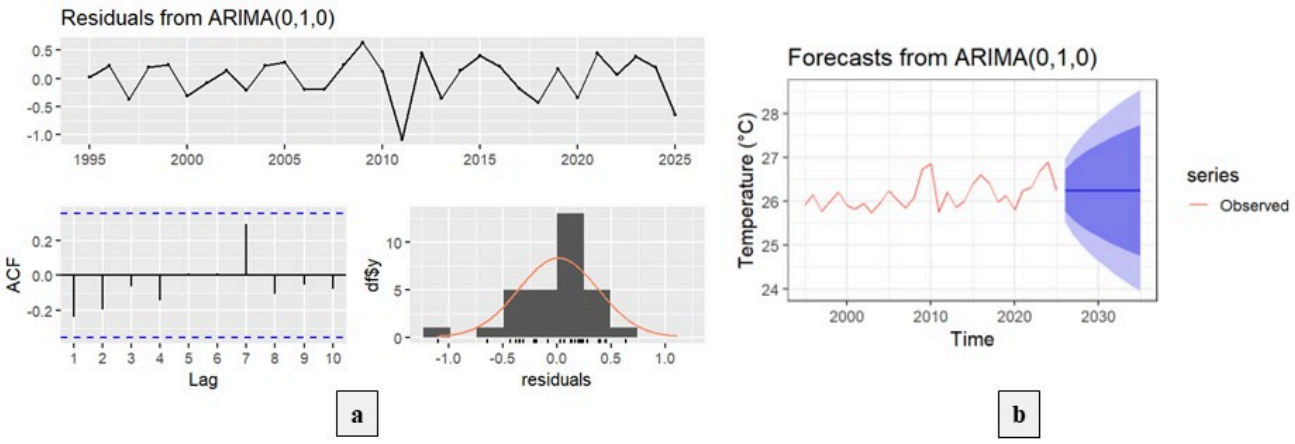


Figure 7

(a) Diagnostic evaluation of the ARIMA model showing residual behaviour and autocorrelation structure. (b) Forecasted annual mean temperature for 2026–2035 with associated prediction intervals.

Supplementary Files

This is a list of supplementary files associated with this preprint. Click to download.

- SupplementaryFileSpatiotemporaltemperaturevariabilityclimateregimeshiftsandthermalriskinBankuraandPuruliadistrictsofWestBengalIndia.docx